

Cdk5 phosphorylation of huntingtin reduces its cleavage by caspases: implications for mutant huntingtin toxicity

Shouqing Luo, Coralie Vacher, Janet E. Davies, and David C. Rubinsztein

Department of Medical Genetics, Cambridge Institute for Medical Research, Addenbrooke's Hospital, Cambridge, CB2 2XY, England, UK

Huntington's disease (HD) is a neurodegenerative disorder caused by an expanded polyglutamine (polyQ) tract in the huntingtin (htt) protein. Mutant htt toxicity is exposed after htt cleavage by caspases and other proteases release NH₂-terminal fragments containing the polyQ expansion. Here, we show htt interacts and colocalizes with cdk5 in cellular membrane fractions. Cdk5 phosphorylates htt at Ser434, and this phosphorylation reduces caspase-mediated htt cleavage at residue 513. Reduced mutant htt cleavage resulting from cdk5

phosphorylation attenuated aggregate formation and toxicity in cells expressing the NH₂-terminal 588 amino acids (htt588) of mutant htt. Cdk5 activity is reduced in the brains of HD transgenic mice compared with controls. This result can be accounted for by the polyQ-expanded htt fragments reducing the interaction between cdk5 and its activator p35. These data predict that the ability of cdk5 phosphorylation to protect against htt cleavage, aggregation, and toxicity is compromised in cells expressing toxic fragments of htt.

Introduction

Huntington's disease (HD) is an autosomal dominant progressive neurodegenerative disorder characterized by abnormal movements, emotional disturbances, and cognitive decline (Rubinsztein and Carmichael, 2003). HD is caused by an expanded CAG trinucleotide repeat tract close to the 5' end of the coding region of the HD gene, which is translated into an abnormally long polyglutamine (polyQ) stretch in the huntingtin (htt) protein. HD is associated with uninterrupted polyQ tracts of 38 or more residues. Genetic and transgenic data suggest that the mutation causes disease predominantly by gain-of-function mechanisms. HD pathology is characterized by intraneuronal aggregates in both the nucleus and in neuronal processes. Exon 1 fragments of htt with expanded polyQ repeats are sufficient to cause cell death in cell models or disease in animal models, and such short fragments show greater toxicity and aggregation compared with full-length mutant constructs (Goldberg et al., 1996; Wellington et al., 2000). Htt can be cleaved by caspases, calpains, and aspartic proteases to form short NH₂-terminal toxic fragments with the expanded polyQ repeats in vitro and in HD brains (Wellington et al., 2000; Kim et al., 2001; Lunkes et

al., 2002). Thus, mutant htt cleavage resulting in toxic fragment production may be an important rate-limiting step in HD pathogenesis. However, the regulation of these events is poorly understood and no previous studies have identified factors other than the proteases themselves that directly influence cleavage.

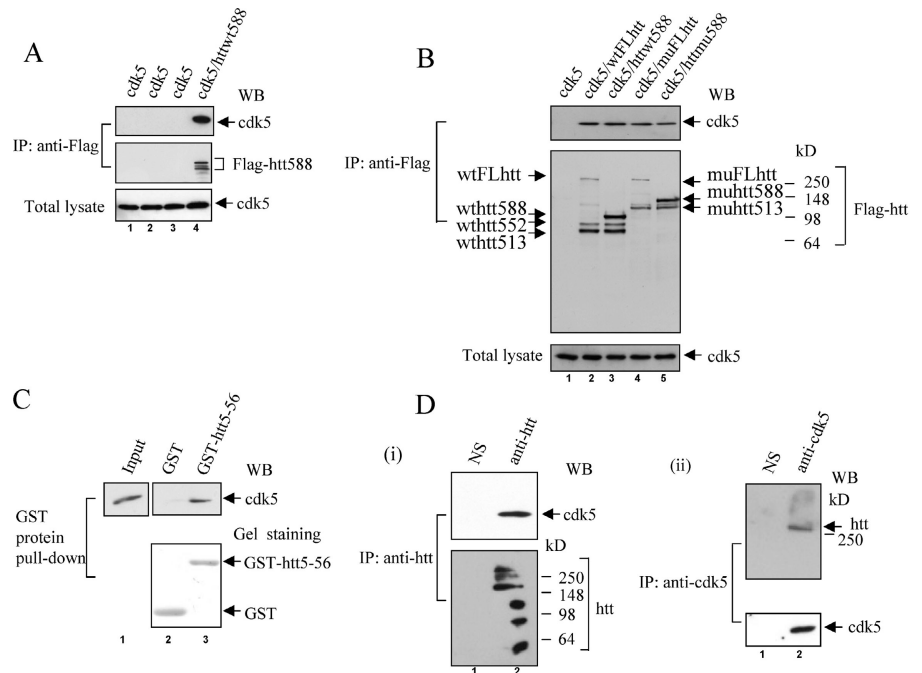
More than 20 htt-interacting proteins have been reported (Harjes and Wanker, 2003). Htt is a predominantly cytoplasmic protein (DiFiglia et al., 1995; Sharp et al., 1995) enriched in membrane fractions (Gutekunst et al., 1995) and associated with microtubules (Hoffner et al., 2002). Htt may have roles in neurotransmission (Glynn et al., 2003), axonal transport, and neuronal positioning (White et al., 1997). We were struck that these functions have also been attributed to another membrane and microtubule-associated protein, cdk5, a member of the small serine/threonine Cdk family. Despite its biochemical and sequence similarities with cdc2 (Meyerson et al., 1992), a role for cdk5 in cell cycle regulation has not yet been identified (Dhavan and Tsai, 2001). Cdk5 phosphorylates more than two dozen proteins with diverse functions (Ino et al., 1994; Dhavan and Tsai, 2001). Although cdk5 is expressed in widespread adult tissues, its activity is highest in neurons because the cdk5-activating proteins p35/p39 are highly expressed in these cells (Tsai et al., 1993; Tang et al., 1995). Both htt and cdk5 are expressed ubiquitously with highest levels in neurons of the CNS, and htt or cdk5 knockout mice show overlapping phenotypes—neuronal cell death and embryonic or perinatal lethality (Zeitlin et al., 1995; Ohshima et al., 1999).

Correspondence to David C. Rubinsztein: dcr1000@cus.cam.ac.uk

Abbreviations used in this paper: cdk5DN, cdk5 dominant-negative; HD, Huntington's disease; htt, huntingtin; httEx1-23Q, htt exon1-23Q; httEx1-74Q, htt exon1-74Q; IP, immunoprecipitation; LM, light membranes; polyQ, polyglutamine.

The online version of this article includes supplemental material.

Figure 1. Htt interacts with Cdk5. (A) COS-7 cells were cotransfected with empty vector and cdk5 (lanes 1–3) or Flag-tagged htt1-588 (htt588) and cdk5 (lane 4). In all experiments, empty vector controls have been performed where appropriate and the amount of empty vector DNA was equivalent to the amount of experimental DNA (in this case, htt588). Cell lysates were immunoprecipitated with anti-Flag. Anti-Flag immunoprecipitates were subjected to immunoblotting with anti-cdk5 (top) or anti-Flag (middle). Total lysates were immunoblotted with anti-cdk5 (bottom). (B) COS-7 cells were cotransfected with empty vector and cdk5 (lane 1); Flag-tagged, wild-type, full-length htt (wtFLhtt) and cdk5 (lane 2); Flag-tagged, wild-type htt588 (httwt588) and cdk5 (lane 3); Flag-tagged, mutant, full-length htt (muFLhtt) and cdk5 (lane 4); and Flag-tagged, mutant htt588 (httmu588) and cdk5 (lane 5), respectively. Cell lysates were immunoprecipitated with anti-Flag and immunoblotted with anti-cdk5 (top) and anti-Flag (middle), respectively. Total lysates were immunoblotted with anti-cdk5 (bottom). (C) Bacterially expressed GST (lane 2) and GST-htt (5–56 aa; lane 3) were incubated with cdk5-transfected COS-7 cell lysate. The cdk5 that associated with GST-htt (5–56 aa) was detected with anti-cdk5. The input signal represents 5% cdk5 in the total cell lysate (lane 1). (D, i) Mouse brain lysate was immunoprecipitated with anti-Flag as a control (NS; lane 1) or anti-htt (181–800; lane 2). Cdk5 associated with htt as shown with anti-cdk5 antibody probing of Western blot of immunoprecipitate (top). (ii) Mouse brain lysate was immunoprecipitated with anti-Myc as a control (NS; lane 1) or anti-cdk5 (C8; lane 2). Htt associated with cdk5 as shown with anti-htt antibody probing of Western blot of immunoprecipitate (top).



Results

Htt interacts with cdk5

The overlapping subcellular localizations and functions of htt and cdk5 and the presence of multiple minimum cdk5 phosphorylation sites within htt led us to test if these proteins interact. Residues 1–588 of htt (htt588) pull down cdk5 (Fig. 1 A) in COS-7 cells. In the middle panel of Fig. 1 A, cleavage products of htt588 are seen, which likely correspond to htt552 and htt513 (Wellington et al., 2000). Using the same coimmunoprecipitation approach, we showed that httwt588 (aa 1–588 of wild-type htt with 17 glutamines-17Q), wtFLhtt (wild-type, full-length htt with 17Q), httmu588 (aa 1–588 of mutant htt with 138Q), and muFLhtt (mutant full-length htt with 138Q) all bound cdk5 (Fig. 1 B). To narrow down the cdk5-binding region of htt, we expressed GST fused to amino acids 5–56 of htt (GST-htt5-56) in *Escherichia coli*, pulled down the recombinant protein with glutathione-sepharose, and incubated it with cdk5-transfected COS-7 cell lysate. Fig. 1 C shows that residues 5–56 of htt bind cdk5. We confirmed the physical interaction of htt and cdk5 in neuronal cells by immunoprecipitating endogenous htt in mouse brain lysate with anti-htt and demonstrating that cdk5 was also pulled down with htt (Fig. 1 D, i). Fig. 1 D (ii) shows the reverse experiment and confirms that endogenous htt can also be immunoprecipitated by anti-cdk5. We could not detect any binding between the cdk5 activator, p35, and htt (unpublished data). These data reveal a selective physical interaction between htt and cdk5.

Htt associates with cdk5 in membrane fraction

Htt is enriched in membrane fractions (Gutekunst et al., 1995). To further investigate if htt and cdk5 interact significantly, we tested if overexpression of htt led to an enrichment of cdk5 in light membranes (LM) such as endosomes and ER vesicles. Cdk5/empty vector or cdk5/htt551 were transfected to COS-7 cells. Fig. 2 A shows similar total cdk5 levels in both cdk5-transfected cells and cdk5/htt-transfected cells (actin, enriched in LM, was used as a protein loading control for total and LM lysates). However, cdk5 levels in LM were much higher in cells where cdk5 (rather than empty vector) was cotransfected with htt. We tested the converse prediction that immunodepletion of htt would reduce cdk5 levels in LM using endogenous htt and cdk5 in mouse brain lysates. In both cytosolic and particularly in LM fractions, cdk5 levels were reduced after htt immunodepletion with anti-htt (181–500 aa; as a function of actin levels; Fig. 2 B). Thus, the reduction of the cdk5 level is a specific consequence of htt immunodepletion, further confirming the interaction between htt and cdk5 in LM. In neuronally differentiated rat pheochromocytoma cells (PC-12 cells), we confirmed colocalization of endogenous htt and cdk5 (Fig. 2 C).

Cdk5 phosphorylates htt in vitro and in vivo

The htt-cdk5 interaction suggested that we should test if htt was a cdk5 substrate. Six minimal cdk5 phosphorylation sites, comprising Ser-Pro or Thr-Pro, were found within htt588. GST-htt588 (but not the control protein, GST) is readily phos-

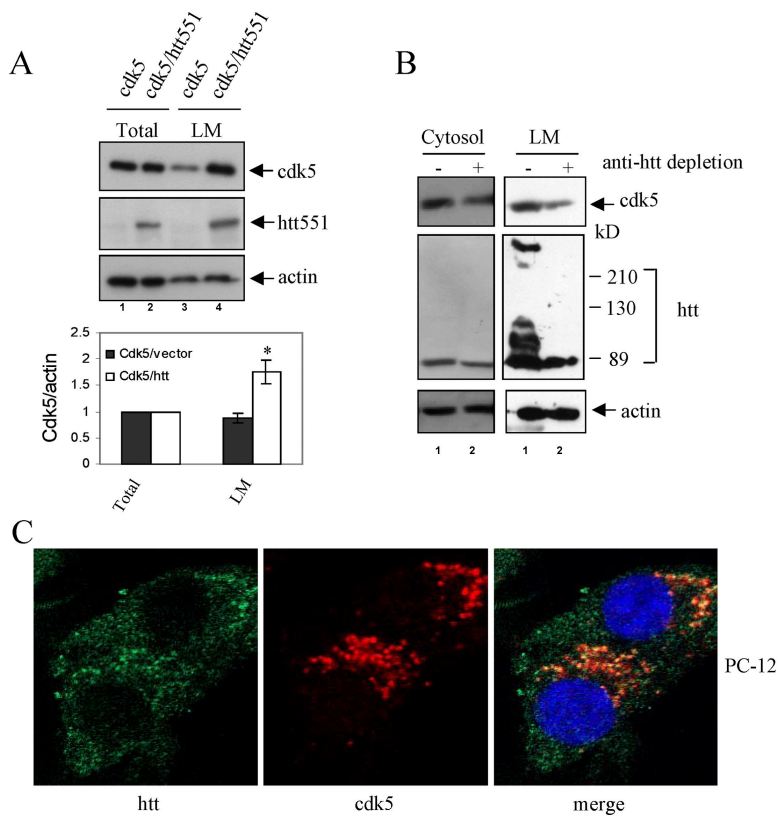


Figure 2. Htt associates with cdk5 at LM. (A) Cdk5 was cotransfected with empty vector/cdk5 (2:1) or Flag-htt1-551 (htt551)/cdk5 (2:1) in COS-7 cells. After 24 h, transfected cells were harvested. Light membranes (LM) (including endosomes and all ER vesicles) were isolated. Total cellular (lanes 1 and 2) and LM (lanes 3 and 4) lysates were resolved by SDS-PAGE and transferred to PVDF membrane, and then probed with anti-cdk5 (top), anti-Flag (middle), and anti-actin (bottom). The blots were quantified with Chemilmager. The ratios of cdk5/actin in total lysates are set as 1. The relative values of cdk5/actin in LM are shown. Three independent experiments were performed. Error bars are SD; *, $P = 0.01$. (B) Mouse brain lysate was immunodepleted with anti-Flag for control (lane 1) or anti-htt (lane 2). The lysate was separated as cytosolic and LM fractions. Cytosolic and LM fractions were resolved by 10% SDS-PAGE and transferred to PVDF membranes. Anti-cdk5 (top), anti-htt (middle), and anti-actin (bottom) were probed for cdk5, htt, and actin, respectively. (C) PC-12 cells were induced to differentiate with 100 ng/ml NGF for 3 d. Confocal immunofluorescence of PC-12 cells: green, anti-htt, Alexa 488; red, anti-cdk5, Alexa 594; blue, nuclei.

phorylated by recombinant p35-cdk5 complex in vitro. (Fig. 3 A). Next, we immunoprecipitated p35-cdk5 complexes from transfected COS-7 cells and incubated these complexes with either httwt588 or httmu588 immunoprecipitated from COS-7 cells. In vitro phosphorylation assays showed that p35-cdk5 could phosphorylate both httwt588 and httmu588 to similar extents (Fig. 3 B). In PC-12 cells, cdk5 activity dramatically increases after NGF differentiation (Harada et al., 2001). To test if htt is phosphorylated by cdk5 in vivo, we differentiated

PC-12 cells with NGF and treated cells with the cdk5 inhibitor roscovitine or DMSO, and then pulled down the endogenous htt with anti-htt. Serine phosphorylation of htt was assessed with the antiphosphoserine antibody 16B4. As Fig. 3 C shows, htt phosphorylation can be detected after differentiation but was abolished with roscovitine (which inhibits cdk5). In vitro kinase assays using histone H1 as a substrate were used to confirm that roscovitine is a potent inhibitor of cdk5 under these conditions (Fig. 3 C).

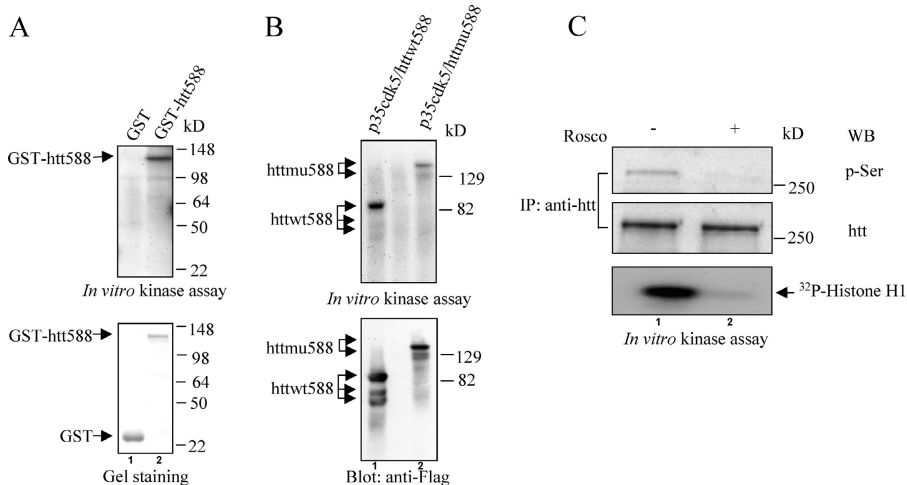
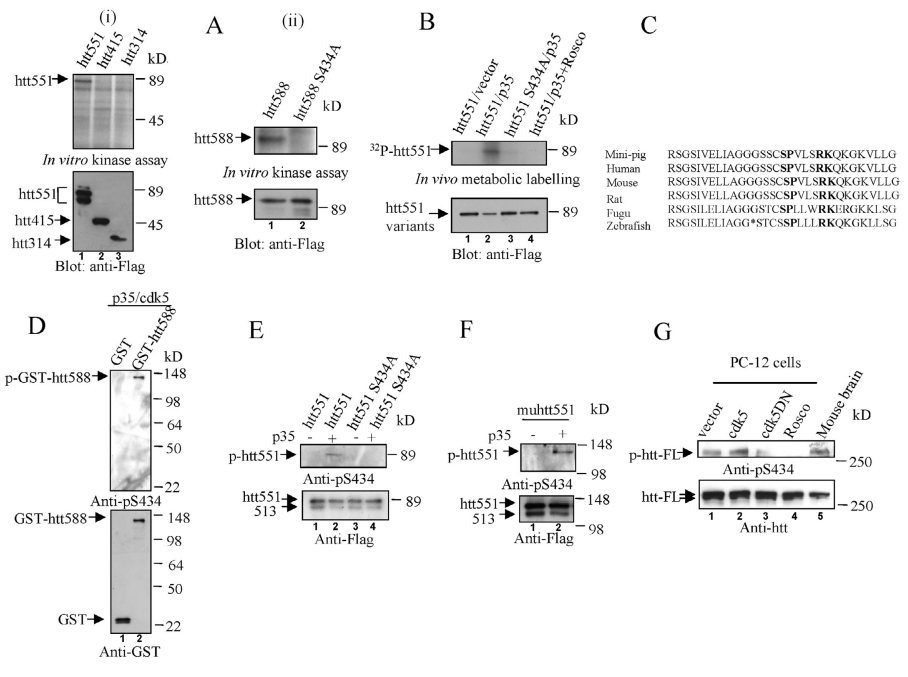


Figure 3. Cdk5 phosphorylates htt in vitro and in vivo. (A) GST and GST-tagged htt1-588 (GST-htt588) (wild-type) were purified from *E. coli*. Both proteins were phosphorylated by 0.1 μ g of p35-cdk5 complexes. Top panel shows phosphorylated GST (lane 1) and GST-htt588 (lane 2). Bottom panel shows purified GST (lane 1) and GST-htt588 (lane 2). (B) p35-cdk5 was cotransfected to COS-7 cells. We immunoprecipitated p35-cdk5 with anti-cdk5. Httwt588 or httmu588 were pulled down with anti-Flag from distinct COS-7 cells transfected with these constructs. The figure shows in vitro kinase assays (top) and anti-Flag blot (bottom) from p35-cdk5 incubated with httwt588 and γ -[32 P]ATP (lane 1) and p35-cdk5 incubated with httmu588 and γ -[32 P]ATP (lane 2). The mixtures were resolved with 10% SDS-PAGE, and then transferred to PVDF membrane and subjected to autoradiography (top). The PVDF membrane

was blotted with anti-Flag (bottom). (C) PC-12 cells were starved for 24 h, and then induced to differentiate with 100 ng/ml NGF for 48 h. Cells were treated with 20 μ M of the cdk5 inhibitor roscovitine (Rosco) or DMSO (control) when cells were induced to differentiate with NGF. After 48 h of treatment, PC-12 cells were lysed in buffer A containing phosphatase inhibitors. Htt was immunoprecipitated with anti-htt antibody, 2166, and then detected with the antiphosphoserine antibody 16B4 (top) and anti-htt (middle). p35-cdk5 complex was pulled down from the differentiated PC-12 cells and an in vitro kinase assay was performed in the presence of DMSO (lane 1) or roscovitine (lane 2) using histone H1 as a substrate (bottom).

Figure 4. **Cdk5 phosphorylates htt at Ser434 in vitro and in vivo.**

(A, i) htt1-551 (htt551), htt1-415 (htt415), and htt1-314 (htt314) were immunoprecipitated with anti-Flag from COS-7 cells, and then γ -[32 P]ATP and 0.1 μ g of recombinant p35-cdk5 complexes were added to htt551 (lane 1), htt415 (lane 2), and htt314 (lane 3) to phosphorylate these htt variants. The mixtures were subjected to SDS-PAGE and transferred to PVDF membrane, subjected to autoradiography (top), and blotted with anti-Flag (bottom). (ii) htt1-588 (htt588; lane 1) and htt588 S434A mutant (htt588 S434A; lane 2) were pulled down, phosphorylated (top), and blotted with anti-Flag (bottom) as above. Note that only htt forms with S434 (lane 1) were efficiently phosphorylated. (B) Htt551/empty vector (lane 1), htt551/p35 (lane 2 and 4), and htt551 S434A/p35 (lane 3) were cotransfected into cdk5-expressing HeLa cells. After 24 h, cells were labeled with [32 P]orthophosphate for 3 h, and one of the htt551/p35 transfections (lane 4) was treated with 20 μ M of the cdk5 inhibitor roscovitine (Rosco) during this process. Htt551 was pulled down with anti-Flag and subjected to SDS-PAGE and transferred to PVDF membrane for autoradiography (top) and immunoblotting with anti-Flag.



(D) Purified GST or GST-htt588 were phosphorylated by p35-cdk5 complex in vitro as described in Materials and methods. 1/100 of the mixtures were subjected to SDS-PAGE and Western blot using phospho-htt antibody, pS434 (top), and anti-GST. (E) Htt551/empty vector (lane 1), htt551/p35 (lane 2), htt551 S434A/empty vector (lane 3), and htt551 S434A/p35 (lane 4) were transfected into HeLa cells. After 24 h, cells were harvested, lysates were subjected to SDS-PAGE, transferred to PVDF membrane, and then probed with anti-pS434 (top). The same membrane was probed with anti-Flag (bottom) after stripping. (F) Htt551-138Q (muhtt) was cotransfected with empty vector (lane 1) or p35 (lane 2). After 24 h, cell lysates were subjected to Western blot and probed with anti-pS434 (top) and anti-Flag (bottom). (G) 5 μ g of empty vector, cdk5, and cdk5DN were cotransfected to PC-12 cells in 10-cm dishes with 1 μ g EGFP. The transfected cells were starved for 24 h and treated with NGF for 4 h. FACS was used to sort GFP-positive (i.e., transfected) cells. Those GFP-positive cell lysates were subjected to Western blot probed with anti-pS434 (top) and anti-htt (bottom), respectively. Newborn mouse brain lysate (lane 5) was probed with anti-pS434 (top) and anti-htt (bottom).

Cdk5 phosphorylates htt at Ser 434 in vitro and in vivo

We mapped the cdk5 phosphorylation site(s) by first testing p35-cdk5 phosphorylation of different truncated htt fragments in vitro. Fig. 4 A (i) suggests the phosphorylation site(s) may be between aa 551 and 415, as phosphorylation was observed with htt551 but not with htt415 or htt314. We mutagenized the potential cdk5 phosphorylation sites within this region. When Ser 434 (S434) was mutated to Ala, cdk5 failed to phosphorylate htt588 in vitro (Fig. 4 A, ii), suggesting that S434 is the only cdk5 phosphorylation site in htt588. We then tested if htt S434 was phosphorylated in vivo. Htt551/empty vector, htt551/p35, and htt551 S434A/p35 were cotransfected into HeLa cells, which express cdk5 but not the activators like p35/p39. After 32 P metabolic labeling, htt551 was phosphorylated only in the presence of p35 (a cdk5-specific activator), confirming the specificity of the reaction to cdk5 kinase activity. Consistent with this specificity, the phosphorylation of htt was inhibited by roscovitine. Mutation of htt S434 to A also prevented phosphorylation in vivo, which is consistent with our in vitro data suggesting that this was the phosphorylation site in vivo (Fig. 4 B). This consensus cdk5 phosphorylation site is conserved in htt orthologues across many vertebrates (Fig. 4 C).

To further confirm that htt is phosphorylated by cdk5 in vivo, we developed an anti-htt-pS434 antibody (anti-pS434; see Materials and methods). To test the antibody, we first phos-

phorylated either GST or GST-htt588 using p35-cdk5 complex in vitro, and then probed gels of the reaction products with anti-pS434. Anti-pS434 detected phospho-GST-htt588 (rather than GST) that had an electrophoretic mobility similar to the GST-htt588; comparable amounts of GST and GST-htt588 were confirmed by anti-GST probing (Fig. 4 D). As htt can be phosphorylated at S434 in HeLa cells in the presence of cdk5 activity (Fig. 4 B), we tested S434 phosphorylation in HeLa cells using the anti-pS434 antibody. When htt551 or htt551 S434A were cotransfected with either empty vector or p35 into HeLa cells, anti-pS434 only detected htt phosphorylation when cdk5 was activated (in the presence of p35) and required S at residue 434, consistent with Fig. 4 B (Fig. 4 E). Fig. 4 F shows that mutant polyQ-expanded htt551 (muhtt551) was phosphorylated at S434 in HeLa cells in the presence of, but not the absence of, p35. Thus, anti-pS434 recognizes phosphorylated htt and only recognizes the specific band when htt is phosphorylated at residue 434. To further show that htt is phosphorylated by cdk5 in vivo, we first transfected PC-12 cells with empty vector (Fig. 4 G, lane 1), cdk5 (Fig. 4 G, lane 2), and cdk5 dominant-negative form (cdk5DN; Fig. 4 G, lane 3) or treated with the cdk5 inhibitor roscovitine (Fig. 4 G, lane 4). The cells were then starved for 24 h and induced with NGF, and transfected cells were sorted with FACS. In cdk5-transfected cells, phosphorylation of endogenous full-length htt slightly increased, but in cdk5DN transfected cells, the phosphorylation is markedly reduced

compared with empty vector transfected cells, and in the roscovitine-treated cells, the phosphorylation is fully disabled (Fig. 4 G). These data also confirm that anti-pS434 can specifically recognize cdk5-phosphorylated forms of full-length htt. Anti-pS434 identified a band of the same mobility as the roscovitine/cdk5DN-sensitive band seen in the PC-12 cells in newborn mouse brain, suggesting that endogenous mouse htt is phosphorylated at S434 (Fig. 4 G, lane 5).

Cdk5 phosphorylation of mutant htt reduces its toxicity

To investigate if cdk5 could modulate mutant htt toxicity, we transfected httmu588 (httmu588 [138Q] with empty vector), httmu588/p35 (httmu588 with p35), httmu588 S434A (httmu588 S434A with empty vector), or httmu588 S434A/p35 (httmu588 S434A with p35) into SK-N-SH (neuroblastoma) cells, which express cdk5 but not the activators like p35/p39 (Fig. 5 A). Activation of endogenous cdk5 kinase activity in these cells by p35 reduced the proportions of cells with aggregates or cell death in the cells expressing httmu588 but did not reduce either the proportions of cells with aggregates or cell death in cells expressing httmu588 S434A, the nonphosphorylatable httmu588 form (Fig. 5 A). Thus, activation (by p35) of cdk5 activity is required in order for it to protect against the toxicity of httmu588 in neuronal cells. Furthermore, this is not a nonspecific protective effect of cdk5 activation but requires S at residue 434 in httmu588.

Cdk5 phosphorylation of htt reduces its cleavage by caspases

We considered that p35–cdk5 may protect against httmu588 by modulating its turnover, but this hypothesis was not supported by our initial experiments (unpublished data). Because cdk5 phosphorylation of httmu551 was associated with a reduction of its cleavage product htt 513 (Fig. 4 F), we tested if p35–cdk5 phosphorylation modulated htt cleavage. Because htt cleavage at sites close to S434 is mediated by caspases, we established assays for htt cleavage in HeLa cells treated with low doses of the caspase-inducing drug staurosporine. We transfected p35 into HeLa cells to activate cdk5 kinase activity. Fig. 5 B shows that staurosporine treatment results in cleavage of htt551 (e.g., Fig. 5 B, lanes 5 and 6). The cleavage of htt551 (as judged by the ratio of htt551 to 513) in the cells with p35 transfection (Fig. 5 B, lane 2) was obviously less than that in cells without p35 transfection (Fig. 5 B, lane 6). Also, p35 expression does not alter htt551 expression (unpublished data). Although p35–cdk5 activity regulated htt551 cleavage induced by staurosporine, it did not reduce staurosporine-induced cleavage of the htt551 S434A mutant (Fig. 5 B, lanes 4 and 8). Thus, htt551 cleavage is specifically regulated by p35–cdk5 acting at S434. Some htt551 cleavage occurred in the absence of staurosporine and p35 (Fig. 5 B). This result may be due to low levels of active caspases (e.g., resulting from transfection), although we cannot exclude a role for other proteases.

We tested if p35–cdk5 regulated cleavage of mutant htt. Fig. 5 C shows that httmu551 cleavage (Fig. 5 C, lanes 1 and 2)

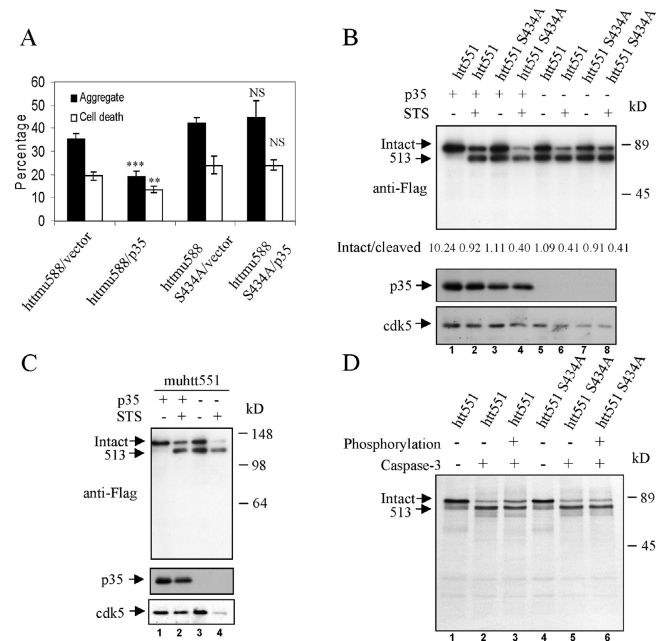
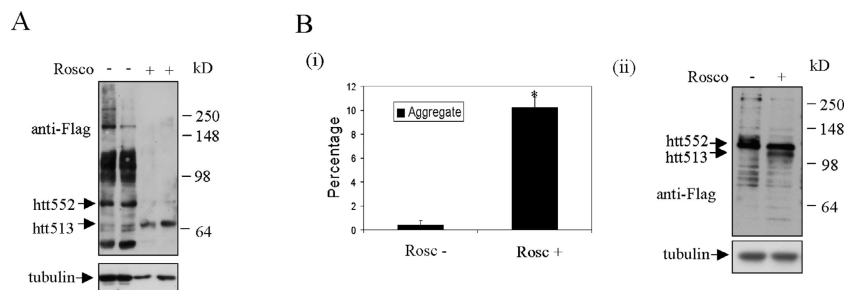


Figure 5. Cdk5-phosphorylating htt blocks caspase cleavage and regulates mutant htt toxicity. (A) Httmu588/vector, httmu588/p35, and httmu588 S434A/vector, and httmu588 S434A/p35 were transfected to cdk5-expressing neuroblastoma SK-N-SH cells. After 48 h, cells were fixed and immunostained with anti-Flag and p35 antibodies. Htt-expressing cells were scored for the presence of aggregates and abnormal nuclei. Data are from three independent experiments. Each experiment was performed in triplicate. Error bars represent SD. ***, $P < 0.0001$; **, $P < 0.001$. (B) p35 was cotransfected with htt551 (lanes 1 and 2) or htt551 S434A (lanes 3 and 4), or empty vector was cotransfected with htt551 (lanes 5 and 6) or htt551 S434A (lanes 7 and 8) into HeLa cells. After 24 h, cells were treated with $1 \mu\text{M}$ staurosporine (STS) for 0 (lanes 1, 3, 5, and 7) or 6 h (lanes 2, 4, 6, and 8). Cell lysates were resolved with 10% SDS-PAGE and transferred to PVDF membrane for Western blotting. The variation in the amount of htt expressed in this transient transfection experiment can vary from well to well depending on the transfection efficiency in the specific well (as well as survival when treated with STS). We are primarily concerned with the proportion of the protein that is cleaved. Quantitation of the intact/cleaved(513) htt ratios from of the scanned original gel is shown. The phenomena shown in this figure were reproduced in independent experiments. (C) p35 was cotransfected with muhtt551 (lanes 1 and 2), or empty vector was cotransfected with htt551 (lanes 3 and 4) into cdk5-expressing HeLa cells. After 24 h, cells were treated with $1 \mu\text{M}$ staurosporine (STS) for 0 (lanes 1 and 3) or 6 h (lanes 2 and 4). Cell lysates were resolved with 10% SDS-PAGE and transferred to PVDF membrane for Western blot. (D) Htt551 and htt551 S434A were in vitro translated with ^{35}S -labeling. The in vitro-translated htt551 (lane 3) and htt551 S434A (lane 6) were phosphorylated in vitro in the presence of recombinant p35–cdk5 complex and ATP- γ -S. The unphosphorylated (lane 2) and phosphorylated htt551 (lane 3) and unphosphorylated (lane 5) and phosphorylated htt551 S434A (lane 6) were subjected to caspase-3 cleavage (100 ng/ml). 10% SDS-PAGE was performed. Data show a representative of three independent experiments.

was consistently much less in p35-expressing cells, compared with cells not transfected with p35 (Fig. 5 C, lanes 3 and 4) in either staurosporine-treated or untreated conditions. Staurosporine-induced htt551 cleavage in cell models is caspase-dependent, as cleavage of htt551 was effectively prevented by the pan-caspase inhibitor Z-VAD-fmk (unpublished data). Because mutant htt cleavage enhances its aggregate formation and toxicity, these data can account for the protective effects observed against httmu588 by p35–cdk5 (Fig. 5 A).

Figure 6. Inhibition of cdk5 activity promotes htt cleavage, and mutant htt aggregate formation in differentiated htt stable PC-12 cells. (A) Wild-type, full-length htt PC-12 cells were differentiated with 100 ng/ml NGF for 48 h. 1 μ g/ml doxycycline was added to induce htt expression for 5 d. At same time, indicated samples in duplicate were also treated with 20 μ M of the cdk5 inhibitor roscovitine. Cells were harvested and subjected to 7.5% SDS-PAGE. Anti-Flag (M2) was used for Western blot. This antibody detects a 3 \times Flag tag at the NH₂-terminal of the htt transgene. (B) Mutant full-length htt PC-12 cells were differentiated with 100 ng/ml NGF for 48 h. 1 μ g/ml doxycycline was added to induce htt expression for 5 d. At the same time as inducing transgene expression, cells were also treated with 20 μ M of the cdk5 inhibitor roscovitine, where indicated. Cells were fixed and anti-Flag (M2) was used for immunocytochemistry. This antibody detects a 3 \times FLAG tag at the NH₂-terminal of the htt transgene. (i) The proportions of cells with aggregates are shown. Experiment was performed in triplicate. Error bars represent SD. *, $P < 0.01$. (ii) Mutant, full-length htt PC-12 cells were differentiated with NGF, induced with doxycycline, and treated with roscovitine as wild-type, full-length htt PC-12 cells. Cells were harvested and subjected to 10% SDS-PAGE. Anti-Flag (M2) was used for Western blot. This antibody detects a 3 \times Flag tag at the NH₂-terminal of the htt transgene.



Because Wellington et al. (1998, 2000) reported that htt can be cleaved by caspase-3 at D513, we tested if cdk5 phosphorylation of htt changed its susceptibility to caspase-3 cleavage in vitro. In vitro-translated ³⁵S-labeled htt551 was phosphorylated in vitro in the presence of recombinant p35-cdk5 and ATP- γ -S, which can phosphorylate htt551. The use of ATP- γ -S ensures stability of the phosphorylated site, as the resulting thio-phosphorylation is resistant to phosphatase attack. Cdk5-phosphorylated htt551 (Fig. 5 D, lane 3) is cleaved less by caspase-3 compared with htt551 that has not been cdk5 phosphorylated (Fig. 5 D, lane 2) or htt551 S434A with or without cdk5-p35 phosphorylation (showing the effect is dependent on the presence of htt S434; Fig. 5 D). Quantification of Fig. 5 D revealed that cdk5 phosphorylation of htt551 increased the ratio of htt551 to htt513 by 1.7-fold in the presence of caspase-3, whereas there was no obvious effect of this phosphorylation in the htt551 S434A mutant (under the same conditions). The phosphorylation probably does not have a more pronounced effect in this experiment, as it is very likely that only a proportion of the molecules are stably phosphorylated (and thus protected from cleavage) under in vitro conditions. Thus, cdk5 phosphorylation of htt prevents its cleavage by caspases and can account for activated cdk5 inhibiting httmu588-induced cell death and aggregation. Because htt phosphorylation by cdk5 prevented its cleavage by caspases in vitro, it is likely that this effect is regulated by phosphorylation itself rather than by interaction of other proteins at the phosphorylation site.

To confirm that cdk5 activity is an important regulator of full-length htt cleavage in vivo, we studied neuronally differentiated PC-12 cells (Sugars et al., 2004), which express either NH₂-terminal Flag-tagged wild-type or mutant, full-length htt under the control of a doxycycline-responsive promoter (Tet-On). We can detect NH₂-terminal cleavage products of these transgenes specifically using an anti-Flag antibody in these cell lines. The transgene expression levels in these cells is similar to the endogenous htt (Sugars et al., 2004). We used these cells to test our prediction that inhibition of cdk5 activity with its inhibitor roscovitine would result in more transgene cleavage at residue 513. Compared with untreated cells, roscovitine-treated NGF-differentiated cells produced more of the caspase cleavage fragment, htt513 (Fig. 6 A). The ratio of htt552 to htt 513

was dramatically reduced in the roscovitine-treated cells, which is consistent with greater cleavage at amino acid 513 in the absence of cdk5 activity. In stable inducible, neuronally differentiated PC-12 cells expressing mutant 138Q full-length transgenes, enhanced htt cleavage would be predicted to result in more aggregates, as aggregation is enhanced by short NH₂-terminal htt products, compared with longer fragments. Consistent with our previous data showing that cdk5-mediated phosphorylation reduces htt cleavage at D513, aggregate formation was substantially increased in neuronally differentiated PC-12 cells treated with roscovitine while expressing the transgene, compared with untreated cells (Fig. 6 B, i and ii). Compared with untreated cells, roscovitine treatment of these cells produced more of the caspase-cleavage fragment htt513 (Fig. 6 B), and the ratio of htt552 to htt 513 was dramatically reduced in the roscovitine-treated cells, which is consistent with greater cleavage at amino acid 513 in the absence of cdk5 activity. Roscovitine was not toxic to PC-12 cells under these conditions (unpublished data). We could not evaluate mutant htt-induced cell death in this model as cell death rates are very low in this cell model expressing mutant full-length htt (Sugars et al., 2004).

Cdk5 activity is reduced in HD transgenic mouse brains

Because cdk5 activity is protective against mutant htt cleavage and toxicity, we investigated if this activity was altered in a mouse model of HD expressing the first 171 residues of htt with expanded polyQs (Schilling et al., 1999). Surprisingly, the specific activity of cdk5 immunoprecipitated from brains of mice carrying the mutant transgene was significantly lower than that (of comparable amounts of cdk5) from wild-type littermates (Fig. 7 A). However, p35 levels were not reduced in brain lysates from the mutant HD mice (Fig. 7 B). Furthermore, cdk5 and p35 were not sequestered into either cytosolic or nuclear htt aggregates in vivo. Samples from human HD brains and HD transgenic mouse brains (and relevant non-HD controls) were analyzed using both peroxidase and immunofluorescence detection systems and no aggregates staining for either cdk5 or p35 were seen, whereas convincing aggregate staining was seen with both antiubiquitin and anti-htt antibodies (unpublished data).

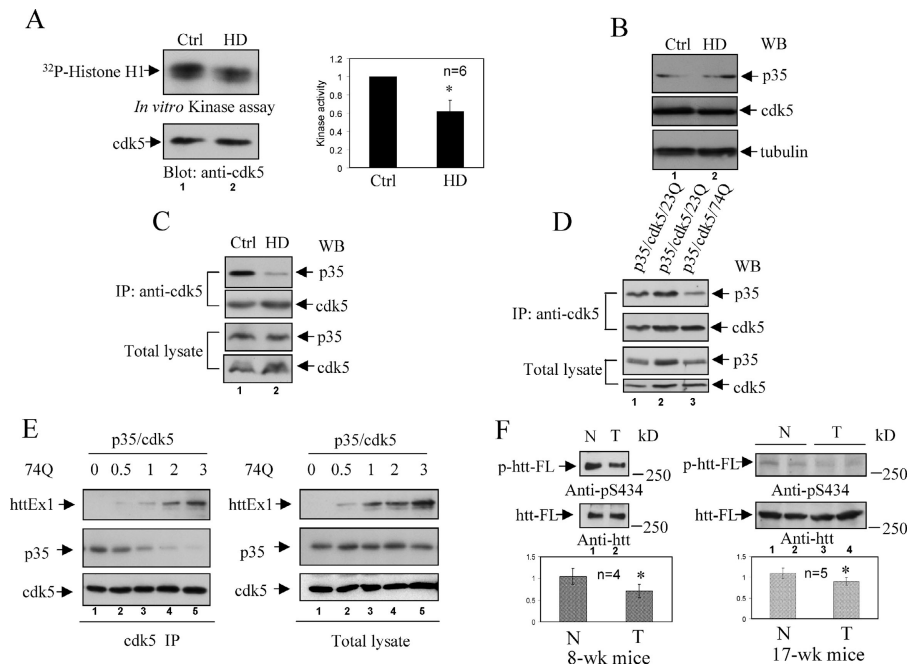


Figure 7. Mutant htt impairs cdk5 activity by interfering p35-cdk5 interaction. (A) Cdk5 was pulled down from the lysates of wild-type littermate control (Ctrl; lane 1) or HD (lane 2) mice whole brains (12 wk). Histone H1 was used as a substrate for kinase assays. Radiophotographs and Western blots were quantified. Six independent experiments were performed. Error bars represent SD. *, $P < 0.05$. Note that kinase activity is expressed as a function of cdk5 levels (specific activity). (B) Whole brain lysates of 13-wk wild-type littermate control (Ctrl; lane 1) and HD (lane 2) mice were subjected to SDS-PAGE, and Western blots were probed successively with anti-p35 (top), -cdk5 (middle), and -tubulin (bottom panel) antibodies. (C) Anti-cdk5 (β 3, monoclonal) was used to pull down p35 from 13-wk-old wild-type littermate control (lane 1) and HD (lane 2) mouse whole brain lysates. Anti-p35 (C-19, polyclonal) was used to detect p35 (top). After stripping, the same membrane was probed with anti-cdk5 (C8, polyclonal) to measure cdk5 levels (second panel). P35 (third) and cdk5 (bottom) levels in total p35/cdk5/GFP-httEx1-23Q (lane 1) and p35/cdk5/GFP-httEx1-74Q (lane 3) transfected COS-7 cell lysates are shown. Data show a representative experiment from four independent experiments. (E) p35-cdk5 (0.75 μ g each) were cotransfected with 0 (lane 1), 0.5 (lane 2), 1 (lane 3), 2 (lane 4), and 3 μ g httEx1-74Q (lane 5), respectively. Note that the total amount of DNA transfected was kept constant by adding empty vector DNA, where necessary. After 48 h, anti-cdk5 was used to immunoprecipitate p35 in each transfected cell. IP products (left) and total cell lysates (right) were detected with anti-GFP, anti-p35, and anti-cdk5, respectively. (F, left) 8-wk-old HD (lane 2) and nontransgenic (lane 1) mouse whole brain lysates were subjected Western blot and probed with anti-pSer434 (top) and anti-htt (bottom). One of the phtt/htt ratios was set as 1 and data were quantified. Error bars represent SD. *, $P < 0.05$. (right) 17-wk-old HD (lanes 3 and 4) and nontransgenic (lanes 1 and 2) mouse whole brain lysates (40 μ g) were subjected to Western blot and probed with anti-pS434 (top) and anti-htt (bottom). One of the phtt/htt ratios was set as 1. Western blot was quantified. Error bars represent SD. *, $P < 0.05$.

experiments. (D) Anti-cdk5 (β 3, monoclonal) was used to pull down p35 from p35/cdk5/GFP-httEx1-23Q (1:1:2) (lane 1) and p35/cdk5/GFP-httEx1-74Q (1:1:2) (lane 3) transfected COS-7 cell lysates. Anti-p35 (C-19, polyclonal) was used to detect p35 (top). After stripping, the same membrane was probed with anti-cdk5 (C8, polyclonal) to measure cdk5 levels (second panel). P35 (third) and cdk5 (bottom) levels in total p35/cdk5/GFP-httEx1-23Q (lane 1) and p35/cdk5/GFP-httEx1-74Q (lane 3) transfected COS-7 cell lysates are shown. Data show a representative experiment from four independent experiments. (E) p35-cdk5 (0.75 μ g each) were cotransfected with 0 (lane 1), 0.5 (lane 2), 1 (lane 3), 2 (lane 4), and 3 μ g httEx1-74Q (lane 5), respectively. Note that the total amount of DNA transfected was kept constant by adding empty vector DNA, where necessary. After 48 h, anti-cdk5 was used to immunoprecipitate p35 in each transfected cell. IP products (left) and total cell lysates (right) were detected with anti-GFP, anti-p35, and anti-cdk5, respectively. (F, left) 8-wk-old HD (lane 2) and nontransgenic (lane 1) mouse whole brain lysates were subjected Western blot and probed with anti-pSer434 (top) and anti-htt (bottom). One of the phtt/htt ratios was set as 1 and data were quantified. Error bars represent SD. *, $P < 0.05$. (right) 17-wk-old HD (lanes 3 and 4) and nontransgenic (lanes 1 and 2) mouse whole brain lysates (40 μ g) were subjected to Western blot and probed with anti-pS434 (top) and anti-htt (bottom). One of the phtt/htt ratios was set as 1. Western blot was quantified. Error bars represent SD. *, $P < 0.05$.

Because htt interacts with cdk5, we hypothesized that the polyQ expansion may reduce cdk5 activity by impairing its interaction with p35. Fig. 7 C shows that much less p35 was pulled down by anti-cdk5 from HD compared with wild-type littermate brain lysate, although comparable amounts of cdk5 were pulled down in the two samples, supporting our hypothesis that mutant htt impairs the p35-cdk5 interaction. Next, we used GFP-htt exon1-23Q (GFP-httEx1-23Q) and GFP-htt exon1-74Q (GFP-httEx1-74Q) in cellular models to confirm the data from HD mice because htt exon1 is sufficient to bind to cdk5. Fig. 7 D shows cdk5 pulled down significantly less p35 in the presence of GFP-httEx1-74Q, compared with cdk5 in the presence of GFP-httEx1-23Q. However, comparable amounts of p35 and cdk5 were seen in the total lysates, and similar levels of cdk5 were immunoprecipitated in cells expressing 23Q or 74Q (Fig. 7 D, lanes 1 and 3). To confirm that polyQ-expanded htt impeded the p35-cdk5 interaction, we cotransfected p35-cdk5 and increasing amounts of httEx1-74Q into COS-7 cells, and then anti-cdk5 was used to pull down p35 and httEx1-74Q in cell lysates (Fig. 7 E). The levels of p35 that were pulled down by cdk5 decreased with the increasing expression of httEx1-74Q.

Next, we tested if endogenous htt phosphorylation was affected in our HD mice that express the first 171 residues of mutant htt because cdk5 activity is reduced in these mice (Fig. 7 A). Htt S434 phosphorylation (phospho-htt/total htt ratio)

was significantly reduced in 8- (presymptomatic) or 17-wk-old (symptomatic) HD mouse brain lysates, compared with nontransgenic age-matched littermates (Fig. 7 F; by 33% and 17%, respectively). The apparent differences in the reduction in htt phosphorylation at 8 and 17 wk may simply be because the experiments at these time points were performed at different times and on different blots.

Htt588 or full-length htt stabilizes p35-cdk5 interaction and expanded polyQ of mutant htt decreases this stabilization

Because htt toxicity is believed to be exposed after cleavage, we tested if mutant htt588 mutant full-length htt reduced the p35-cdk5 interaction. Surprisingly, we found that both httwt588 and httmu588 (Fig. 8 A) and full-length wthtt and muhtt (Fig. 8 B) increased the p35-cdk5 interaction. However, mu588 and mutant full-length were less effective than their wt counterparts (Fig. 8, A and B). However, exon1-23Q does not significantly alter the affinity of p35-cdk5 interaction, whereas exon1-74Q interferes with the interaction, which is consistent with Fig. 7 (C-E). The cleavage of full-length htt and htt588 may explain why the mutant forms of these proteins are less effective than their wild-type counterparts at stabilizing the cdk5-p35 interaction because mutant htt exon 1 impairs p35-cdk5 binding. In addition, we consistently observed that more mutant htt than wild-type protein was pulled

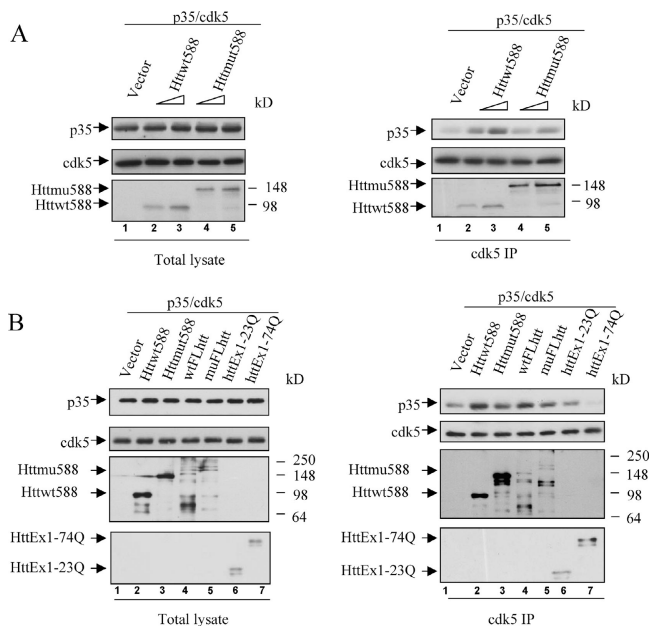


Figure 8. Htt588 or full-length htt stabilizes p35–cdk5 interaction, and expanded polyQ of mutant htt compromises this stabilization. (A) p35–cdk5 (0.75 μ g each) were cotransfected into HeLa cells with 1 μ g of empty vector (lane 1), 0.5 μ g httwt588 (+0.5 μ g of empty vector, to ensure similar amounts of DNA transfected in all lanes) (lane 2), 1 μ g httwt588 (lane 3), 0.5 μ g hitmu588 (+0.5 μ g empty vector) (lane 4), and 1 μ g hitmu588 (lane 5). After 24 h, cell lysates were subjected to IP with mouse anti-cdk5 (J3). The IP products were probed with anti-p35, anti-cdk5, and anti-Flag (for htt), respectively. Data represent a representative of experiments repeated four times with similar trends. (B) p35–cdk5 (0.75 μ g each) were cotransfected with empty vector (lane 1), httwt588 (lane 2), hitmu588 (lane 3), wFLhtt (lane 4), muwFLhtt (lane 5), httEx1-23Q (lane 6), and httEx1-74Q (lane 7) into HeLa cells; the ratio of p35/cdk5/htt is 1:1:2. The cell lysates were immunoprecipitated with anti-cdk5. The IP products were then probed with anti-p35, anti-cdk5, anti-Flag (for htt588 and full-length htt), and anti-GFP (for GFP-httEx1). Similar results were observed in another two independent experiments.

down using anti-cdk5 (J3) (Fig. 8), which we did not observe using anti-Flag antibody. The stronger binding is not nonspecific because neither httwt588 nor hitmu588 were pulled down by anti-cdk5 in httwt588- or hitmu588-only transfected cell lysates. (Please note that it is almost impossible to achieve equal transfection efficiencies of exon 1 htt, htt588, and full-length htt in the same experiment due to the vastly different sizes of the expression vectors.)

The data in cell and mouse models suggest that the interaction between cdk5 and its activator p35 is impaired by NH₂-terminal mutant htt, which accounts for the reduced cdk5 activity we observed in HD mouse brains. Thus, the ability of cdk5 to prevent htt cleavage by caspases may be partially abrogated in HD mouse brains.

Discussion

Here, we show that htt selectively interacts with cdk5 but not its activator, p35. Recent data showed that Akt and the serum- and glucocorticoid-induced kinase SGK phosphorylate htt at serine 421 and regulate its toxicity (Humbert et al., 2002; Rangone et al., 2004), although the mechanisms remain un-

known. We show that htt is a cdk5 substrate at S434 and phosphorylation at this site reduces htt cleavage at D513, although we cannot exclude other cdk5 phosphorylation sites beyond htt588. The exact mechanism whereby phosphorylation leads to decreased caspase cleavage is still not clear; however, a likely explanation is that the negative charge (and possibly altered structure) conferred by phosphorylation inhibits the accessibility of caspases to their recognition site. Protein phosphorylation regulating caspase-mediated cleavage happens in many proteins. Casein kinase I and II phosphorylation of Bid regulates its cleavage by caspase-8 (Desagher et al., 2001), ERK phosphorylation of caspase-9 regulates its processing (Allan et al., 2003), and MAPK phosphorylation of the androgen receptor enhances its cleavage by caspase-3 (LaFevre-Bernt and Ellerby, 2003).

Cdk5-mediated htt phosphorylation appears to be an important regulator of mutant htt cleavage, aggregation, and toxicity. Our data are consistent with those of Wellington et al. (2000, 2002), who provided biochemical and in vivo data supporting cleavage of mutant htt at caspase sites in HD. Htt phosphorylation at S434 provides a novel means of regulating an early and likely rate-limiting event in HD pathogenesis. Although our data implicate caspases as important and possibly rate-limiting components of the htt cleavage cascade, it is important to consider this in the context of other proteases contributing to the process, like calpains, aspartic proteases, and possibly other as yet uncharacterized proteases.

Cdk5 activity and phosphorylation of endogenous htt at S434 were reduced in htt 171 HD transgenic mice, and our data suggest that this results from mutant htt reducing the association between cdk5 and its activator p35. The interaction between p35 and cdk5 may be affected by the polyQ expansion in mutant htt, which appears to interact more strongly with cdk5 compared with wild-type htt. These data predict that the ability of cdk5 phosphorylation to protect against htt cleavage, aggregation, and toxicity is compromised in cells expressing toxic fragments of htt.

Our data raise the speculation that there may be a positive feedback loop acting to enhance the progression of mutant htt cytotoxicity in humans. The idea of a positive feedback loop is supported by our observation that mutant exon1 fragments reduce cdk5–p35 interactions (compared with either wild-type exon 1 or empty vector control), whereas longer products (1–588 or full length) increase the stability of the p35–cdk5 interaction compared with empty vector. This finding is seen with both mutant and wild-type forms of htt 1–588 or the full-length protein. It is interesting to contrast the cdk5 situation with our previous observation of mutant htt interacting with the mTOR kinase (Ravikumar et al., 2004). Although mutant htt results in loss of function of both kinases, in the mTOR case, the interaction is mainly due to a direct sequestration effect in aggregates and leads to some effects that are protective. As discussed in the previous paragraph, the inhibition of cdk5 activity is mediated by soluble mutant htt and is likely to be deleterious. Nevertheless, this raises the possibility that truncated forms of mutant htt may bind preferentially to several kinases and cause diverse physiological changes.

Although the reduction of htt phosphorylation at the cdk5 site in HD mice brain may appear to be modest, this reflects the average of a heterogeneous population of neurons with different susceptibilities to mutant htt toxicity and different stages of the pathogenic process. Indeed, it is quite feasible that even a small perturbation resulting in a positive feedback process would have major consequences in the context of decades in human HD. Once a certain level of cleavage has occurred, this would release a toxic product that would inhibit cdk5 activity, which would in turn enhance cleavage. A positive feedback loop is one type of process that can account for the fact that most HD patients are clinically unaffected and have normal brain morphology/volume until a decade or so before the disease manifests in middle age and that the rate of neurodegeneration seems much faster after onset than before onset. Such a feedback loop would also be accelerated in rare HD patients who have inherited two expanded alleles (“homozygotes”) and may account for the observation that the progression of disease appears to be more rapid in such cases, compared with heterozygotes who have similar ages at onset (Squitieri et al., 2003). In addition to these direct effects of cdk5 on htt, it is possible that reduced cdk5 activity may also have other consequences for HD pathogenesis.

Materials and methods

Generation of anti-pSer434-htt antibody

In brief, the Ser434-phosphorylated peptide of htt, C-GGSSpSPVLSR (Sigma-Aldrich), was used to immunize two rabbits. Serum was collected from the two rabbits after four injections. The serum was passed through unphosphorylated peptide-conjugated Sepharose (Pierce Chemical Co.). The flow-through was passed over phosphorylated peptide-conjugated Sepharose. The phosphorylated antibody, designated as pS434, was eluted with 0.1 M glycine, pH 2.3.

Immunoprecipitation (IP)

IP was performed using buffer A (20 mM Tris-HCl, pH 7.2, 2 mM MgCl₂, 150 mM NaCl, 5 mM NaF, 1 mM Na₂VO₄, 0.5% NP-40, and protease inhibitor cocktail [Roche]). Cells were lysed in buffer A for 20 min on ice, followed by centrifugation at 13,000 g for 15 min. Primary antibodies (or anti-Flag M2-agarose affinity gel and anti-cdk5 [J3]-coupling gel [Pierce Chemical Co.]) were added to a final concentration of 5 µg/ml and incubated for 2 h to overnight at 4°C. Anti-mouse or -rabbit IgG agarose were added to the mixture and incubated at 4°C for 1 h. After three washings, IP products were either directly boiled in Laemmli buffer or eluted with 0.1 M glycine, pH 2.3, and then boiled in Laemmli buffer and subjected to PVDF membrane transfer and Western blot.

GST pull-down assay

GST or GST-htt (aa5-56) expressed in BL21 (DE3) were adsorbed to glutathione-agarose beads for 1 h after 3× PBS washing. The bound GST or GST-htt (aa 5–56) were incubated with the lysate of COS-7 cells transfected with cdk5 in buffer A for 2 h at 4°C, and then washed three times in buffer A. The bound proteins were resolved by SDS-PAGE and transferred to PVDF membrane. The blot was probed with anti-cdk5.

LM and cytosol fractionation

Cells or mouse brains were suspended in STM buffer (10 mM KCl, 10 mM Tris, pH 7.9, 1 mM DTT, 250 mM sucrose, and protease inhibitors cocktail) at 4°C, incubated for 20 min on ice with swirling, and lysed by 20 strokes in a Dounce homogenizer. The homogenate was clarified at 15,000 g for 15 min at 4°C, and the supernatant was centrifuged for 1 h at 100,000 g at 4°C. The second supernatant and pellet were collected as cytosol and LM, respectively. The LM include Golgi, endosomes, and all ER vesicles. LM were lysed in buffer A.

Quantification of autoradiographs

To quantify cdk5 level in LM in the presence or absence of htt, the specified bands were analyzed by Chemilmager (Alpha Innotech Co.). Cdk5/

actin (for LM cdk5 level) of total lysates were set as 1, and the relative values of LM cdk5/actin was analyzed.

Cellular fragmentation of mouse brains

Mouse brains were suspended in buffer A, incubated for 20 min on ice with swirling, and lysed by 20 strokes in a Dounce homogenizer. The homogenate was clarified at 15,000 g for 10 min at 4°C, and the supernatant was collected for Western blot or IP.

In vitro kinase assay

Kinase assays were performed by washing immunoprecipitates twice with buffer A and twice with kinase buffer (50 mM HEPES, pH 7.0, 10 mM MgCl₂, and 1 mM DTT). p35-cdk5 complexes were incubated with 50 µl of kinase buffer containing the substrate 5 µCi γ-[³²P]ATP at RT for 30 min. After boiling, mixtures were separated by SDS-PAGE and transferred to PVDF membrane.

Metabolic labeling

HeLa cells were transfected with htt551 for 24 h. The cells were incubated with 0.3 mCi/ml [³²P]orthophosphate (Amersham Biosciences) in phosphate-free DME for 4 h at 37°C. The cells were lysed in 0.5 ml of buffer A. Htt was immunoprecipitated using anti-Flag, separated by SDS-PAGE, transferred to PVDF membrane, and analyzed by autoradiography. The membrane was subsequently probed with anti-Flag.

Estimation of cell death and aggregates

To measure cell death or aggregates, ~200 transfected cells (as judged by anti-Flag immunocytochemistry) were counted in multiple random visual fields per slide. All coverslips were scored with the observer blinded to the identity of the slides. Cells were analyzed using a fluorescent microscope (model Eclipse E600; Nikon). The figures show data from representative experiments in triplicate. Cell death was monitored by scoring the transfected cells with apoptotic nuclear morphology—fragmented or pyknotic nuclei. Cells were counted as aggregate-positive if one or several aggregates were visible within a cell. P-values were determined by unconditional logistical regression analysis by using the general loglinear option of 9.1 software (SPSS).

In vitro translation and cleavage

In vitro translations were performed in TNT-coupled reticulocyte lysate systems following Promega's instruction. 2 µl of ³⁵S-labeled products were phosphorylated in the presence of cdk5-p35 complex and ATP-γ-S (if necessary) and cleaved by 100 ng/ml caspase-3 in cleavage buffer (50 mM HEPES, pH 7.2, 50 mM NaCl, 0.1% Chaps, 10 mM EDTA, 5% glycerol, and 10 mM DTT) for 1 h at 37°C. The cleaved products were subjected to 10% SDS-PAGE. Films were exposed after gel drying. We divided the in vitro translated htt into three identical aliquots. One aliquot was phosphorylated as described in the previous section and one was mock-phosphorylated by leaving out the cdk5-p35. These aliquots were treated identically with the relevant caspase and compared with the third aliquot that was not treated with caspase (or phosphorylated), the control uncleaved protein.

Online supplemental material

Details of vector construction, antibodies and reagents, cell culture and treatments, and immunocytochemistry and microscopy are available online. Online supplemental material is available at <http://www.jcb.org/cgi/content/full/jcb.200412071/DC1>.

We thank Drs. M.R. Hayden and C. Wellington for generous gifts of full-length htt-17Q and htt-138Q. We are grateful to the Medical Research Council (Programme Grant with Professor Steve Brown) and the Wellcome Trust (Senior Clinical Fellowship) for giving funding to D.C. Rubinsztein and his group. D.C. Rubinsztein is on the Scientific Advisory Board of Daniolabs and has grant funding from Wyeth and SienaBiotech for projects unrelated to this paper.

Submitted: 10 December 2004

Accepted: 24 March 2005

References

- Allan, L.A., N. Morrice, S. Brady, G. Magee, S. Pathak, and P.R. Clarke. 2003. Inhibition of caspase-9 through phosphorylation at Thr 125 by ERK MAPK. *Nat. Cell Biol.* 5:647–654.
- Desagher, S., A. Osen-Sand, S. Montessuit, E. Magnenat, F. Vilbois, A. Hochmann, L. Journot, B. Antonsson, and J.C. Martinou. 2001. Phosphoryla-

tion of bid by casein kinases I and II regulates its cleavage by caspase 8. *Mol. Cell.* 8:601–611.

- Dhavan, R., and L.H. Tsai. 2001. A decade of CDK5. *Nat. Rev. Mol. Cell Biol.* 2:749–759.
- DiFiglia, M., E. Sapp, K. Chase, C. Schwarz, A. Meloni, C. Young, E. Martin, J.P. Vonsattel, R. Carraway, S.A. Reeves, et al. 1995. Huntingtin is a cytoplasmic protein associated with vesicles in human and rat brain neurons. *Neuron.* 14:1075–1081.
- Glynn, D., R.A. Bortnick, and A.J. Morton. 2003. Complexin II is essential for normal neurological function in mice. *Hum. Mol. Genet.* 12:2431–2448.
- Goldberg, Y.P., D.W. Nicholson, D.M. Rasper, M.A. Kalchman, H.B. Koide, R.K. Graham, M. Bromm, P. Kazemi-Esfarjani, N.A. Thornberry, J.P. Vaillancourt, and M.R. Hayden. 1996. Cleavage of huntingtin by apopain, a proapoptotic cysteine protease, is modulated by the polyglutamine tract. *Nat. Genet.* 13:442–449.
- Gutekunst, C.A., A.I. Levey, C.J. Heilman, W.L. Whaley, H. Yi, N.R. Nash, H.D. Rees, J.J. Madden, and S.M. Hersch. 1995. Identification and localization of huntingtin in brain and human lymphoblastoid cell lines with anti-fusion protein antibodies. *Proc. Natl. Acad. Sci. USA.* 92:8710–8714.
- Harada, T., T. Morooka, S. Ogawa, and E. Nishida. 2001. ERK induces p35, a neuron-specific activator of Cdk5, through induction of Egr1. *Nat. Cell Biol.* 3:453–459.
- Harjes, P., and E.E. Wanker. 2003. The hunt for huntingtin function: interaction partners tell many different stories. *Trends Biochem. Sci.* 28:425–433.
- Hoffner, G., P. Kahlem, and P. Djian. 2002. Perinuclear localization of huntingtin as a consequence of its binding to microtubules through an interaction with beta-tubulin: relevance to Huntington's disease. *J. Cell Sci.* 115:941–948.
- Humbert, S., E.A. Bryson, F.P. Cordelieres, N.C. Connors, S.R. Datta, S. Finkbeiner, M.E. Greenberg, and F. Saudou. 2002. The IGF-1/Akt pathway is neuroprotective in Huntington's disease and involves Huntingtin phosphorylation by Akt. *Dev. Cell.* 2:831–837.
- Ino, H., T. Ishizuka, T. Chiba, and M. Tatibana. 1994. Expression of CDK5 (PSSALRE kinase), a neural cdc2-related protein kinase, in the mature and developing mouse central and peripheral nervous systems. *Brain Res.* 661:196–206.
- Kim, Y.J., Y. Yi, E. Sapp, Y. Wang, B. Cuiffo, K.B. Kegel, Z.H. Qin, N. Aronin, and M. DiFiglia. 2001. Caspase 3-cleaved N-terminal fragments of wild-type and mutant huntingtin are present in normal and Huntington's disease brains, associate with membranes, and undergo calpain-dependent proteolysis. *Proc. Natl. Acad. Sci. USA.* 98:12784–12789.
- LaFevre-Bernt, M.A., and L.M. Ellerby. 2003. Kennedy's disease. Phosphorylation of the polyglutamine-expanded form of androgen receptor regulates its cleavage by caspase-3 and enhances cell death. *J. Biol. Chem.* 278:34918–34924.
- Lunke, A., K.S. Lindenberg, L. Ben-Haiem, C. Weber, D. Devys, G.B. Landwehrmeyer, J.L. Mandel, and Y. Trotter. 2002. Proteases acting on mutant huntingtin generate cleaved products that differentially build up cytoplasmic and nuclear inclusions. *Mol. Cell.* 10:259–269.
- Meyerson, M., G.H. Enders, C.L. Wu, L.K. Su, C. Gorka, C. Nelson, E. Harlow, and L.H. Tsai. 1992. A family of human cdc2-related protein kinases. *EMBO J.* 11:2909–2917.
- Ohshima, T., E.C. Gilmore, G. Longenecker, D.M. Jacobowitz, R.O. Brady, K. Herrup, and A.B. Kulkarni. 1999. Migration defects of *cdk5^{-/-}* neurons in the developing cerebellum is cell autonomous. *J. Neurosci.* 19:6017–6026.
- Rangone, H., G. Poizat, J. Troncoso, C.A. Ross, M.E. MacDonald, F. Saudou, and S. Humbert. 2004. The serum- and glucocorticoid-induced kinase SGK inhibits mutant huntingtin-induced toxicity by phosphorylating serine 421 of huntingtin. *Eur. J. Neurosci.* 19:273–279.
- Ravikumar, B., C. Vacher, Z. Berger, J.E. Davies, S. Luo, L.G. Oroz, F. Scaravilli, D.F. Easton, R. Duden, C.J. O'Kane, and D.C. Rubinsztein. 2004. Inhibition of mTOR induces autophagy and reduces toxicity of polyglutamine expansions in fly and mouse models of Huntington disease. *Nat. Genet.* 36:585–595.
- Rubinsztein, D.C., and J. Carmichael. 2003. Huntington's disease: molecular basis of neurodegeneration. *Expert Rev. Mol. Med.* 2003:1–21.
- Schilling, G., M.W. Becher, A.H. Sharp, H.A. Jinnah, K. Duan, J.A. Kotzok, H.H. Slunt, T. Ratovitski, J.K. Cooper, N.A. Jenkins, et al. 1999. Intracellular inclusions and neuritic aggregates in transgenic mice expressing a mutant N-terminal fragment of huntingtin. *Hum. Mol. Genet.* 8:397–407.
- Sharp, A.H., S.J. Loev, G. Schilling, S.H. Li, X.J. Li, J. Bao, M.V. Wagster, J.A. Kotzok, J.P. Steiner, A. Lo, et al. 1995. Widespread expression of Huntington's disease gene (IT15) protein product. *Neuron.* 14:1065–1074.
- Squitieri, F., C. Gellera, M. Cannella, C. Mariotti, G. Cislighi, D.C. Rubinsztein, E.W. Almqvist, D. Turner, A.C. Bachoud-Levi, S.A. Simpson, et al. 2003. Homozygosity for CAG mutation in Huntington disease is associated with a more severe clinical course. *Brain.* 126:946–955.
- Sugars, K.L., R. Brown, L.J. Cook, J. Swartz, and D.C. Rubinsztein. 2004. Decreased cAMP response element-mediated transcription: an early event in exon 1 and full-length cell models of Huntington's disease that contributes to polyglutamine pathogenesis. *J. Biol. Chem.* 279:4988–4999.
- Tang, D., J. Yeung, K.Y. Lee, M. Matsushita, H. Matsui, K. Tomizawa, O. Hatase, and J.H. Wang. 1995. An isoform of the neuronal cyclin-dependent kinase 5 (Cdk5) activator. *J. Biol. Chem.* 270:26897–26903.
- Tsai, L.H., T. Takahashi, V.S. Caviness Jr., and E. Harlow. 1993. Activity and expression pattern of cyclin-dependent kinase 5 in the embryonic mouse nervous system. *Development.* 119:1029–1040.
- Wellington, C.L., L.M. Ellerby, A.S. Hackam, R.L. Margolis, M.A. Trifiro, R. Singaraja, K. McCutcheon, G.S. Salvesen, S.S. Propp, M. Bromm, et al. 1998. Caspase cleavage of gene products associated with triplet expansion disorders generates truncated fragments containing the polyglutamine tract. *J. Biol. Chem.* 273:9158–9167.
- Wellington, C.L., R. Singaraja, L. Ellerby, J. Savill, S. Roy, B. Leavitt, E. Cattaneo, A. Hackam, A. Sharp, N. Thornberry, et al. 2000. Inhibiting caspase cleavage of huntingtin reduces toxicity and aggregate formation in neuronal and nonneuronal cells. *J. Biol. Chem.* 275:19831–19838.
- Wellington, C.L., L.M. Ellerby, C.A. Gutekunst, D. Rogers, S. Warby, R.K. Graham, O. Loubser, J. van Raamsdonk, R. Singaraja, Y.Z. Yang, et al. 2002. Caspase cleavage of mutant huntingtin precedes neurodegeneration in Huntington's disease. *J. Neurosci.* 22:7862–7872.
- White, J.K., W. Auerbach, M.P. Duyao, J.P. Vonsattel, J.F. Gusella, A.L. Joyner, and M.E. MacDonald. 1997. Huntingtin is required for neurogenesis and is not impaired by the Huntington's disease CAG expansion. *Nat. Genet.* 17:404–410.
- Zeitlin, S., J.P. Liu, D.L. Chapman, V.E. Papaioannou, and A. Efstratiadis. 1995. Increased apoptosis and early embryonic lethality in mice nullizygous for the Huntington's disease gene homologue. *Nat. Genet.* 11:155–163.